Aspects of marginally trapped and antitrapped surfaces in a *D*-dimensional evolving dust model

Konka Raviteja[*] and Sashideep Gutti[†]

Department of Physics, Birla Institute of Technology and Sciences-Pilani, Hyderabad 500078, India

In this paper, we explore the formation of the marginally trapped/ antitrapped surfaces that arise from the evolution of dust in *D*-dimensions with and without the cosmological constant. We obtain analytical expressions for such surfaces. We also derive closed form expressions for the norms of various quantities that decide the Causal nature of the marginally trapped/antitrapped surfaces. We discuss several interesting features of evolution of these surfaces that are significantly different from the four dimensional counterpart. We obtain the expressions for the Ashtekar-Badrikrihnan's area-balance law for dynamical horizon (spacelike surface) tailored for the case of spherically symmetric dust evolution in *D*-dimensions.

I. INTRODUCTION

The black-hole horizon is a very interesting arena where quantum field theory and general relativity come face to face. The relation between the area of the black-hole horizon and its entropy is one of most important developments of recent times and has been a favorite testing ground for various theories of quantum gravity. A study of the dynamics of the horizon evolution is therefore of great importance since one can track the evolution of quantities like entropy and correlate it with the flux of matter or gravitational waves crossing the horizon. The concept of trapping horizons was coined (as against the event horizon) to locally track the evolving horizon by Penrose [1]. Hayward in his paper [2] has refined the concept of trapping horizons based on a $2 + 2$ decomposition framework which introduced various trapped horizons like future outer trapped horizon (FOTH), future inner trapped horizon (FITH), past outer trapped horizon (POTH) and past inner trapped horizon (PITH). Ashtekar, Badrikrishnan *et al.* [3–7] have formulated a closely related notions to Hayward's trapped horizons, which is based on a $3 + 1$ space-time decomposition framework where they have introduced isolated horizons, dynamical horizons, and timelike membranes. The dynamical horizon is defined as a spacelike hypersurface foliated by 2-Spheres such that the expansion for outgoing (k^a) and incoming (l^a) null normal are $\Theta_k = 0$ and $\Theta_l < 0$ respectively on every leaf of the foliation. The area of the dynamical horizon is shown to increase monotonically provided the null energy condition is satisfied. If there is no matter flux or gravitational waves crossing the dynamical horizon then it becomes null and is

called an isolated horizon. Likewise it is shown that one can similarly construct a timelike membrane that arise in cosmological or few cases of gravitational collapse. It is shown in [6] that in contrast to the dynamical horizon case, the area monotonically decreases for a timelike membrane. In the work of Booth *et al.* [8], many possible situations where one can find dynamical horizons, timelike membranes are highlighted and also looked at their causal nature following the prescription given in [9] to classify the horizons as timelike or spacelike. Busso in [10] has introduced a construction for past holographic screen and future holographic screen which are be defined in terms of marginally trapped surfaces (MTS) or marginally antitrapped surfaces (MATS) respectively. Using this construction Busso and Engelhardt in [11,12] have proved a new area law in general relativity where the area of a holographic screen changes monotonically even though the causal nature of the screen (horizon) changes during its evolution.

In this paper, we work with a model [13] where the matter content is pressureless dust in a spherically symmetric arrangement in *D*-dimensions (the Lemaitre-Tolman-Bondi model generalized to *D*-dimensions). This model for matter evolution has the advantage that it is general enough to capture many features of Horizon evolution and is simple enough to yield closed form expressions for various scenarios like FOTH, FITH, POTH, PITH. This can therefore yield the *D*-dimensional versions of various results highlighted in [8,14–16]. The area balance law for dynamical horizon given in $3 + 1$ dimensions is extended to *D* dimensions for a spherical topology, which is applied to this model. The analysis of the model in this paper can be used to represent two situations. First, it can represent the evolution of matter of a star if we put a cut-off for the density at some finite radius. Second, it can be interpreted as a cosmological solution

[*]konka.raviteja@gmail.com
[†]sashideep@hyderabad.bits-pilani.ac.in

(when we set the density to be homogeneous). This analysis is inclusive of the cosmological constant.

In this model, we obtain the general expression Θ_k, Θ_l by defining the outgoing and ingoing null rays in the evolving space-time. Based on the expressions obtained, we can obtain the curve $\Theta_k = 0$ or $\Theta_l = 0$ in the form $f(r, t, D, \Lambda) = $ constant in the relevant time and radial coordinate (t, r) respectively. We evaluate the norm of the vector orthogonal to these curves and from this deduce the signature of the horizon. We show that this is equivalent to the prescription given by Booth *et al.* [8] where the signature of the curves (horizons) is evaluated using the ratio of Lie derivatives of Θ_k and Θ_l. Here we will see that the causal nature of the D-dimensional horizon evolution is indeed richer and more varied compared to the $3 + 1$ scenario. For, e.g., it is well known that the for the case of $3 + 1$ dimensional Oppenheimer-Snyder matter evolution, the MTS is a timelike membrane. We show in the article that in D-dimensional Oppenheimer-Snyder dust evolution, the MTS is timelike for dimension $D < 5$ and is null for $D = 5$ and is space-like for $D > 5$. The causal nature of the horizon becomes more interesting when we analyze the MTS, MATS. We observe that in the evolution of MTS and MATS, the Horizon makes a transition from timelike to spacelike. We show the expressions highlighting these transitions in the article. We show that even though there is transition from timelike to spacelike, the evolution of the Area is strictly monotonic in the time coordinate used in the model (in accordance with the results in [11,12]).

II. HIGHER DIMENSIONAL SPHERICALLY SYMMETRIC DUST EVOLUTION

The general metric for an $(D = n + 2)$ dimensional spherically symmetric spacetime is of the form

$$ds^2 = -e^{\mu(t,r)}dt^2 + e^{\lambda(t,r)}dr^2 + R^2(t,r)d\Omega_n^2 \quad (1)$$

where $d\Omega_n^2$ is the metric on unit n dimensional sphere, t is the time coordinate and r is the comoving radial coordinate. It is easily shown [13] that the g_{00} component of the metric can be chosen to be minus one, i.e., $g_{00} = -1$. The metric then has the following form.

$$ds^2 = -dt^2 + e^{\lambda(t,r)}dr^2 + R^2(t,r)d\Omega^2. \quad (2)$$

For a nonzero cosmological constant ($\Lambda \neq 0$), the Einstein equations are

$$G_{\mu\nu} + \Lambda g_{\mu\nu} = \kappa T_{\mu\nu} \quad (3)$$

here κ is a constant and is related to gravitational constant G_n, ($\kappa = 8\pi G_n$). The matter we are considering here is a pressure less dust hence the only nonzero component of the stress-energy tensor (in the comoving and synchronous

coordinate system) is $T_{00} = \epsilon(t, r)$, where $\epsilon(t, r)$ is the energy density of the dust. With these conditions we get the Einstein equations which are shown in [13] and summarized below

$$G_{00} = \frac{e^{-\lambda}}{R^2}\left[-\Lambda e^\lambda R^2 + \frac{n(n-1)}{2}(e^\lambda(1+\dot{R}^2) - R'^2)\right.$$
$$\left. + \frac{n}{2}RR'\lambda' + \frac{n}{2}(-2RR'' + e^\lambda R\dot{R}\dot{\lambda})\right] = k\epsilon(t,r) \quad (4)$$

$$G_{01} = \frac{n}{2}\frac{(R'\dot{\lambda} - 2\dot{R}')}{R} = 0 \quad (5)$$

$$G_{11} = \frac{1}{R^2}\left[\frac{n(n-1)}{2}(R'^2 - e^\lambda(1+\dot{R}^2))\right.$$
$$\left. + \Lambda e^\lambda R^2 - ne^\lambda R\ddot{R}\right] = 0 \quad (6)$$

$$G_{22} = -\frac{1}{4}e^{-\lambda}[2(n-2)(n-1)(e^\lambda(1+\dot{R}^2) - R'^2)$$
$$- 2(n-1)(2RR'' - RR'\lambda' - e^\lambda(R\dot{R}\dot{\lambda} + 2R\ddot{R}))$$
$$+ e^\lambda R^2(-4\Lambda + \dot{\lambda}^2 + 2\ddot{\lambda})] = 0. \quad (7)$$

The other nonzero relations are given by

$$G_{(j+1j+1)} = \sin^2\theta_{(j-1)}G_{(jj)} \quad (8)$$

where j takes values from 2 to $n + 1$. The expressions for the evolution of matter can be obtained by simplifying the above set of equations. Solving for the G_{01} we get

$$e^\lambda = \frac{R'^2}{1 + f(r)} \quad (9)$$

where $f(r)$ is an arbitrary function called the energy function. Integration of the G_{11} equation after using the above relation gives

$$\dot{R}^2 = f(r) + \frac{2\Lambda}{n(n+1)}R^2 + \frac{F(r)}{R^{(n-1)}} \quad (10)$$

where $F(r)$ is called the mass function. Solving for G_{00} we find

$$\kappa\epsilon(t,r) = \frac{nF'}{2R^nR'}. \quad (11)$$

This gives us the expression for the mass function as

$$F(r) = \frac{2\kappa}{n}\int \epsilon(0,r)r^n dr \quad (12)$$

where $\epsilon(0, r)$ is the initial energy density of the dust and choose that at $t = 0$, $R = r$. We work for the case of

marginally bounded shells of dust where we require that $f(r) = 0$. The result (12) is obtained by keeping the constant value of $f(r) = 0$, and this holds true from here on. Throughout the article we shall assume that $\epsilon > 0$. (weak energy condition is satisfied).

A. Solutions of homogeneous dust evolution

The advantage of the homogeneous case is that the physical radius R (area radius) is separable into a time dependent part and the comoving radius r

$$R(r, t) = a(t)r \tag{13}$$

This model can be used in couple of ways. One is that these solutions can be used to describe cosmological solutions. The other way is that these solutions could represent the generalization of Oppenheimer-Snyder evolution of dust to a general dimension with a cosmological constant. In the latter case the solutions described in this section will work as the interior solutions that need to be matched to an exterior solution (generalization of Schwarzschild solution to higher dimensions including a cosmological constant).

We choose $a(t = 0) = 1$ thus the comoving radius r is equal to the physical radius R (area radius) at initial time ($t = 0$). For a homogeneous dust collapse $\epsilon(t, r)$ is a function only of time t so the initial time density profile of the dust cloud $\epsilon(0, r)$ is taken to be a positive constant which does not depend on the value of r. So the mass function (12) in the homogeneous case is

$$F(r) = \frac{2g}{n(n+1)} r^{n+1} \tag{14}$$

where $g = \kappa \epsilon(0, r)$ and $g > 0$.

Also in the homogeneous case the expression (10) becomes

$$\dot{R}^2 = \frac{2\Lambda}{n(n+1)} R^2 + \frac{2g r^{n+1}}{n(n+1) R^{n-1}} \tag{15}$$

and under the condition of (13) this reduces to

$$\dot{a}(t)^2 = \frac{2\Lambda}{n(n+1)} a(t)^2 + \frac{2g}{n(n+1) a(t)^{n-1}}. \tag{16}$$

In the subsections below, we look at the solutions of (16) for various cases of the cosmological constant being zero, negative and positive.

1. Case of flat spacetime

The equation (16) for flat spacetime is

$$\dot{a}(t)^2 = \frac{2g}{n(n+1) a(t)^{n-1}} \tag{17}$$

For the initial condition that we choose $a(0) = 1$ which means that $R(0, r) = r$, then the solutions for $a(t)$ are

$$\left(1 + \sqrt{\frac{g(n+1)}{2n}} t \right)^{\frac{2}{1+n}} \tag{18}$$

and

$$\left(1 - \sqrt{\frac{g(n+1)}{2n}} t \right)^{\frac{2}{1+n}} \tag{19}$$

2. Case of anti–de Sitter spacetime

The equation (16) for anti–de Sitter spacetime is

$$\dot{a}(t)^2 = \frac{-2\Lambda}{n(n+1)} a(t)^2 + \frac{2g}{n(n+1) a(t)^{n-1}} \tag{20}$$

for the initial condition $a(0) = 1$ the solutions for $a(t)$ are

$$\left(\sqrt{\frac{g}{\Lambda}} \sin \left(\sqrt{\frac{\Lambda(n+1)}{2n}} t + \arcsin \sqrt{\frac{\Lambda}{g}} \right) \right)^{\frac{2}{n+1}} \tag{21}$$

and

$$\left(-\sqrt{\frac{g}{\Lambda}} \sin \left(\sqrt{\frac{\Lambda(n+1)}{2n}} t - \arcsin \sqrt{\frac{\Lambda}{g}} \right) \right)^{\frac{2}{n+1}}. \tag{22}$$

3. Case of de Sitter spacetime

The equation (16) for de Sitter spacetime is

$$\dot{a}(t)^2 = \frac{2\Lambda}{n(n+1)} a(t)^2 + \frac{2g}{n(n+1) a(t)^{n-1}}. \tag{23}$$

The solutions of $a(t)$ for our initial condition $a(0) = 1$ are

$$\left(\sqrt{\frac{g}{\Lambda}} \sinh \left(\sqrt{\frac{\Lambda(n+1)}{2n}} t + \arcsin h \sqrt{\frac{\Lambda}{g}} \right) \right)^{\frac{2}{n+1}} \tag{24}$$

and

$$\left(-\sqrt{\frac{g}{\Lambda}} \sinh \left(\sqrt{\frac{\Lambda(n+1)}{2n}} t - arc \sin h \sqrt{\frac{\Lambda}{g}} \right) \right)^{\frac{2}{n+1}} \tag{25}$$

III. MARGINALLY TRAPPED AND ANTITRAPPED SURFACES

Marginally trapped surfaces (MTS) are defined as codimension 2 sub-manifolds Σ whose expansion of null

congruence Θ_k generated by the outgoing radial null vector k^a vanishes everywhere ($\Theta_k = 0$) on Σ and Θ_l which is expansion of null congruence generated by incoming radial null vector l_a is completely negative on Σ ($\Theta_l < 0$). For these definitions and more see the following references [5,6,8,14,17–22].

Similarly we define marginally antitrapped surfaces (MATS) as codimension 2 submanifolds Ξ whose expansion of incoming radial null congruence Θ_l vanishes everywhere ($\Theta_l = 0$) on Ξ and the expansion of outgoing radial null congruence Θ_k is completely positive on Ξ ($\Theta_k > 0$). These MTS and MATS are also referred to as future and past holographic screens respectively, mostly in the context of holographic theories [11,12,23].

From the metric (2) we have the future outgoing radial null vector as

$$k^a = (1, e^{-(\frac{\lambda}{2})}, 0, 0, 0, \ldots, 0) \tag{26}$$

and the future incoming radial null vector as

$$l^a = (1, -e^{-(\frac{\lambda}{2})}, 0, 0, 0, \ldots, 0) \tag{27}$$

these two future directed radial null vectors are normalized as

$$k^c l_c = k^c l^d g_{cd} = -2$$

and h_{ab} is the induced metric on the marginally trapped or marginally antitrapped surface which is

$$h_{ab} = g_{ab} + \frac{(k_a l_b + l_a k_b)}{(-k^c l^d g_{cd})} = g_{ab} + \frac{1}{2}(k_a l_b + l_a k_b)$$

so the expansion for outgoing bundle of null rays is

$$\Theta_k = h^{ab}\nabla_a k_b = \frac{n}{R}(\dot{R} + e^{-(\frac{\lambda}{2})}R')$$

using Eq. (9) we have

$$\Theta_k = \frac{n}{R}(\dot{R} + 1) \tag{28}$$

similarly the expansion for ingoing bundle of null rays is

$$\Theta_l = h^{ab}\nabla_a l_b = \frac{n}{R}(\dot{R} - e^{-(\frac{\lambda}{2})}R')$$

again using Eq. (9) we have

$$\Theta_l = \frac{n}{R}(\dot{R} - 1). \tag{29}$$

A. Causal nature of the marginally trapped and antitrapped tubes: General D dimensional LTB

The marginally trapped tubes (MTT) or marginally antitrapped tubes (MATT) are codimension 1 submanifolds which are foliated by the marginally trapped or marginally antitrapped surfaces respectively. We look at the causal nature of these tubes formed in the evolution of the dust, these tubes can be timelike (Timelike tubes), spacelike (dynamical horizons) or null (isolated horizons) depending on various situations which emerge [8,14,15]. This is done using two methods, in the first one we calculate the norm of the normal to the tubes in (r, t) plane and use it to classify the causal nature of these tubes (applicable for the case of Spherical Symmetry) while the second one is a standard method used [9] where the ratios of lie derivatives of the expansions are taken which determines the causal nature of the tangent vector to the tube. We use these result to find the causal nature of the tubes that are formed in the dust evolution for the general case

METHOD I: For this model, we have explicit expression for the tubes in the (r, t) plane. If we consider the expression for $\Theta_k = c_1$ where c_1 a constant and using (10) and (28) expressions we get the curve in the (r, t) plane give by

$$\Theta_k = \frac{n}{R}(-\sqrt{\Delta} + 1) = c_1 \tag{30}$$

where

$$\Delta = \frac{2\Lambda}{n(n+1)}R^2 + \frac{F(r)}{R^{(n-1)}}. \tag{31}$$

The norm of the normal to the curve in the (r, t) plane determines the causal nature, so the components of the normal to this curve are

$$n_t = -\frac{n\dot{R}}{R^2}(1 - \sqrt{\Delta}) - \frac{n\dot{\Delta}}{2R\sqrt{\Delta}}$$

and

$$n_r = -\frac{nR'}{R^2}(1 - \sqrt{\Delta}) - \frac{n\Delta'}{2R\sqrt{\Delta}}$$

note that for $c_1 = 0$ this curve indicates the marginally trapped tube. This means for evaluating the norm of this normal we impose the conditions $\dot{R} = -1$, $\Delta = 1$. The norm works out to be,

$$\beta_k = -(n_t)^2 + \frac{(n_r)^2}{R'^2} = \frac{n^2}{4R^2}\left(-\dot{\Delta}^2 + \frac{\Delta'^2}{R'^2}\right) \tag{32}$$

and also using (11) the norm simplifies as,

$$\beta_k = \frac{4\kappa\epsilon R^2}{n^2}\left(\kappa\epsilon + 2\Lambda - \frac{n(n-1)}{R^2}\right). \qquad (33)$$

So the norm β_k is a function of energy density (ϵ) on the tube, the cosmological constant (Λ), the area radius (R) and the number of dimensions ($n = D - 2$).

Now repeating the same exercise for marginally anti-trapped tubes with Θ_l as

$$\Theta_l = \frac{n}{R}(\sqrt{\Delta} - 1) = c_2 \qquad (34)$$

where c_2 is a constant. The norm evaluates to the same expression given by,

$$\beta_l = \frac{4\kappa\epsilon R^2}{n^2}\left(\kappa\epsilon + 2\Lambda - \frac{n(n-1)}{R^2}\right). \qquad (35)$$

Method II: The standard method for determining the causal nature of marginally (anti) trapped tubes was first discussed in [8] and is done by calculation of ratio of Lie derivatives of Θ_k and Θ_l. The signature of quantities α_l and α_k discussed below determines the causal nature of the tangent vectors to the MATT and MTT respectively. The lie derivatives for Θ_k are

$$\begin{aligned}
\text{£}_k\Theta_k &= k^a\nabla_a\Theta_k \\
&= \frac{n}{R^2}\left[\frac{R\dot{\Delta}}{2\sqrt{\Delta}} + \frac{R\Delta'}{2R'\sqrt{\Delta}} - (\dot{R} + 1)(\sqrt{\Delta} + 1)\right]
\end{aligned}$$

$$\begin{aligned}
\text{£}_l\Theta_k &= l^a\nabla_a\Theta_k \\
&= \frac{n}{R^2}\left[\frac{R\dot{\Delta}}{2\sqrt{\Delta}} - \frac{R\Delta'}{2R'\sqrt{\Delta}} - (\dot{R} - 1)(\sqrt{\Delta} + 1)\right].
\end{aligned}$$

The causal nature of the marginally trapped tube is determined by the ratio

$$\alpha_k = \frac{\text{£}_k\Theta_k}{\text{£}_l\Theta_k} \qquad (36)$$

which has to be evaluated at $\Theta_k = 0$ which implies $\dot{R} = -1$ and $\Delta = 1$, we get

$$\alpha_k = \frac{-\kappa\epsilon}{\left(\kappa\epsilon + 2\Lambda - \frac{n(n-1)}{R^2}\right)}. \qquad (37)$$

Similarly the causal nature of the marginally antitrapped tubes is determined by the ratio

$$\alpha_l = \frac{\text{£}_l\Theta_l}{\text{£}_k\Theta_l} \qquad (38)$$

which has to be evaluated at $\Theta_l = 0$ which implies $\dot{R} = 1$ and $\Delta = 1$, we get the α_l ratio to be

$$\alpha_l = \frac{-\kappa\epsilon}{\left(\kappa\epsilon + 2\Lambda - \frac{n(n-1)}{R^2}\right)}. \qquad (39)$$

From Eqs. (33) and (37) it is clear that $\beta_k > 0$ is equivalent to $\alpha_k < 0$ and imply the MTT is timelike also $\beta_k < 0$ is equivalent to $\alpha_k > 0$ and imply the MTT is spacelike. Similarly from (35), (39) when $\beta_l > 0$ ($\alpha_l < 0$) imply MATT is timelike and $\beta_l < 0$ ($\alpha_l < 0$) means MATT is spacelike. The expressions for α_k and α_l match with the results obtained [Eq. (23)] in [15] and [Eq. (2.3)] in [8] where the latter expression involves energy density, pressure and the area. We note that the formula depending on the "area" is valid in four dimensions only and in other dimensions, the expression continues to depend on R^2 which does not have the interpretation of area for the MTT or MATT.

We summarize below the Lie derivatives for MTT ($\Theta_k = 0$)

$$\text{£}_k\theta_k = -\kappa\epsilon \qquad (40)$$

$$\text{£}_l\theta_k = \left(\kappa\epsilon + 2\Lambda - \frac{n(n-1)}{R^2}\right) \qquad (41)$$

and MATT ($\Theta_l = 0$)

$$\text{£}_l\theta_l = -\kappa\epsilon \qquad (42)$$

$$\text{£}_k\theta_l = \left(\kappa\epsilon + 2\Lambda - \frac{n(n-1)}{R^2}\right). \qquad (43)$$

The lie derivatives in Eqs. (41) and (43) are useful in further characterization of the MTT and MATT into outer and inner horizons as defined by Hayward [2].

1. Causal nature of marginally (anti) trapped tubes in homogeneous dust evolution

Here we adapt the expressions derived for the D-dimensional LTB model for the case of homogeneous dust evolution. The mass function for the homogeneous case (14) is of the form

$$F(r) = c_0 r^{n+1} \qquad (44)$$

where $c_0 = 2\kappa\epsilon(0, r)/(n(n+1))$. We further can show using the same relation that the energy density,

$$\kappa\epsilon(t,r) = \frac{n(n+1)c_0}{2a^{n+1}} \tag{45}$$

plugging $\dot{R}^2 = 1$ in the Eq. (10) yields the condition for the MATT in the current context to be,

$$r^2\left[\frac{c_0}{a^{n-1}} + \frac{2\Lambda a^2}{n(n+1)}\right] = 1. \tag{46}$$

The above equation relates the co-moving radius with the scale factor for the horizon. Now substituting the above relation into the expressions for β_k (33) and β_l (35) and simplifying yields the relation,

$$\beta_k = \beta_l = \frac{2\kappa\epsilon}{n}\left(3 - n + \frac{2\Lambda R^2}{n}\right) \tag{47}$$

this is the formula for the norm of the normal to the MTT and MATT that occur in homogeneous dust evolution in terms of the energy density on the tube $(\kappa\epsilon)$, the dimension of the space-time $(D = n + 2)$, the cosmological constant (Λ) and the area radius (R) of MTT or MATT. Similarly computing the lie derivatives for the homogeneous case we get

$$\pounds_k\theta_k = -\kappa\epsilon \tag{48}$$

$$\pounds_l\theta_k = \frac{n}{2R^2}\left(3 - n + \frac{2\Lambda R^2}{n}\right) \tag{49}$$

$$\pounds_l\theta_l = -\kappa\epsilon \tag{50}$$

$$\pounds_k\theta_l = \frac{n}{2R^2}\left(3 - n + \frac{2\Lambda R^2}{n}\right) \tag{51}$$

the formula for α_k and α_l is given by

$$\alpha_k = -\frac{-2\kappa\epsilon R^2}{n}\left(3 - n + \frac{2\Lambda R^2}{n}\right)^{-1} = \alpha_l. \tag{52}$$

B. Marginally trapped surfaces (MTS)

The condition for marginally trapped surface (MTS) is

$$\Theta_k = 0 \quad \text{and} \quad \Theta_l < 0 \tag{53}$$

from the relations (28) and (29) the above conditions imply that

$$\dot{R} = -1 \quad \text{and} \quad \dot{R} < 1 \tag{54}$$

so $\dot{R} = -1$ satisfies both these conditions. This means that for $R(r,t) = r\, a(t)$ we can write comoving radius r for the MTT as function of time

$$r_h = \frac{-1}{\dot{a}(t)} \tag{55}$$

and the areal radius is expressed as

$$R_h(t,r) = -\frac{a(t)}{\dot{a}(t)} \tag{56}$$

From the solutions we got for $a(t)$, we look at the behavior of MTS as they evolve in time t, for the cases where $\Lambda = 0$, > 0 and < 0

1. MTS for flat case

We choose the solution for $a(t)$ for MTS in the case of $\Lambda = 0$ as

$$a(t) = \left(1 - \sqrt{\frac{g(n+1)}{2n}}t\right)^{\frac{2}{1+n}} \tag{57}$$

This solution of $a(t)$ is chosen such that r_h and R_h can have positive values for MTS. We are interested in obtaining the curve in the t–r plane for which $\theta_k = 0$. Using the condition (55) we obtain the expression for r_h as

$$\sqrt{\frac{n(n+1)}{2g}}\left(1 - \sqrt{\frac{g(n+1)}{2n}}t\right)^{\frac{n-1}{n+1}} \tag{58}$$

so we plot r_h versus t for various dimensions $(D = 3 \text{ to } 7)$ is shown in Fig. 1.
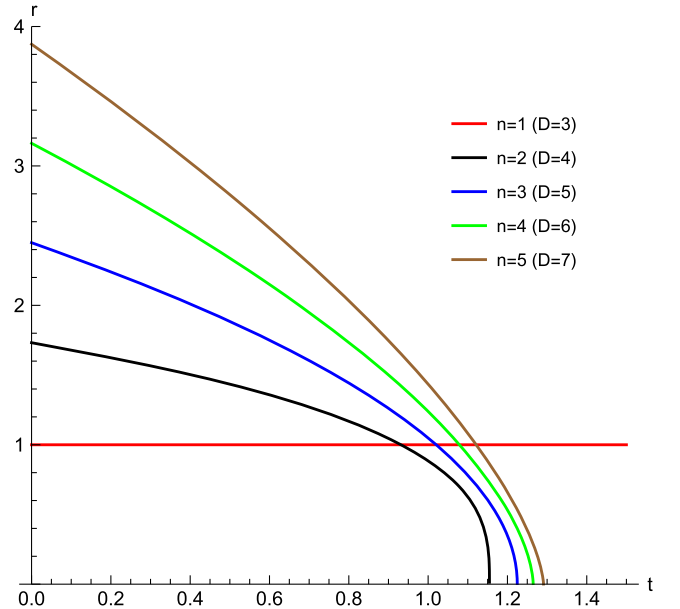

FIG. 1. r_h versus t for MTT with $(\Lambda = 0, g = 1)$.

These graphs represent the MTT which gives the evolution of the MTS in time t as each point on these curves is an MTS and we are tracking these MTT curves from time $t = 0$ to the time when they reach the shell with label $r = 0$ which is a singularity as R also goes to zero here and also the Ricci scalar blows up. We see there is an anomalous curve for $D = 3$ because there are no trapped surfaces in the absence of cosmological constant for the case of $2 + 1$ dimensions as observed in [24]. The line for $D = 3$ represents when the conical defect becomes 2π in the $2 + 1$ dimensional scenario and the relation between the conical defect and the mass function $F(r)$ can be seen in [24,25].

The causal nature of these graphs can be seen from the expression for the norm (47), the sign of β_k is positive for $D < 5$ ($n < 3$) implying that the MTT is timelike. It becomes null for $D = 5$ ($n = 3$) where the MTT curve coincides with an ingoing null ray, this is an example where the horizon need not be isolated and can still be null. The MTT is uniformly spacelike for $D > 5$ ($n > 3$). We note that for $D = 4$, the MTT is timelike as seen in [8,14]. In the above graph and the graphs that follow, we present the evolution for a certain time interval which happens here only due to the matter flux. The MTS unlike the event horizon is defined locally without a need for the complete global description. We look at the evolution for the Areal Radius for these MTS using (57) which gives us a linear relation between R_h and time (t) given by,

$$\sqrt{\frac{n(n+1)}{2g}} - \frac{(n+1)t}{2}. \qquad (59)$$
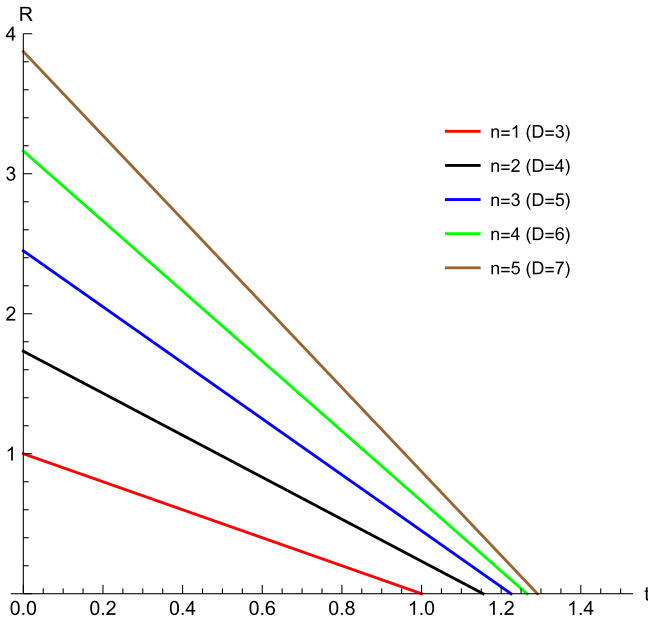
The plot for R versus t is shown in Fig. 2.

FIG. 2. R versus t for MTT with $(\Lambda = 0, g = 1)$.

Note that R decreases monotonically with the coordinate time t for all the cases irrespective of the number of dimensions and whether the MTT is spacelike or timelike. The areal radius becomes zero at a finite time t indicating singularity formation hence we don't need to extend the solutions beyond $R = 0$, this hold true for all the cases to follow.

These MTT can be further characterized as FOTH or FITH as introduced by Hayward [2] and outlined in [16]. Looking at the sign of $\pounds_l\Theta_k = n(3-n)/2R^2$, we see that for $D > 5(n > 3)$ the sign is negative indicating that the horizon is an outer horizon (FOTH). For $D < 5$, we see that the horizon is an inner horizon (FITH). The nontrivial case is for $D = 5$ where the horizon is null but not isolated. We comment about the inner and outer classification for $D = 5$ in a note at the end of the section.

2. MTS for AdS case

The solution for the scale factor a(t) in Homogeneous dust evolution for the case with negative cosmological constant is given by

$$\left(-\sqrt{\frac{g}{\Lambda}}\sin\left(\sqrt{\frac{\Lambda(n+1)}{2n}}t - \arcsin\sqrt{\frac{\Lambda}{g}}\right)\right)^{\frac{2}{n+1}}. \qquad (60)$$

One can see that the solutions are oscillatory in nature. The evolution in the graphs given below represent the situation where the matter cloud contracts from a given initial configuration and collapses to a point. One can also consider the reversed situation where the matter expands out from a point (this situation is dealt with when analyzing the MATS case). We therefore present a segment of the entire evolution of the cloud for the purpose of tracking the evolution of MTS. The negative cosmological constant provides an extra "attractive force" on the shells and the cloud collapses more efficiently than the previous case where the cosmological constant is kept to zero. The evolution of MTS as a curve in the (t, r) plane where the comoving radius r_h is given by

$$-\sqrt{\frac{n(n+1)}{2\Lambda}}\frac{1}{a(t)}\tan\left(\sqrt{\frac{\Lambda(n+1)}{2n}}t - \arcsin\sqrt{\frac{\Lambda}{g}}\right). \qquad (61)$$

The plot for r_h versus t is shown in Fig. 3.
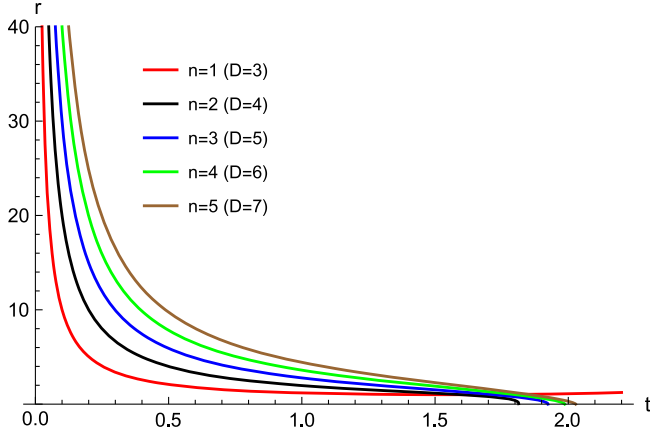
FIG. 3. r versus t for MTT with ($\Lambda = 1$, $g = 1$).

For $D \geq 4$, we can see that at time t equal to zero, the comoving radius that has just for trapped is the intercept the curve makes on the r axis. For all the comoving radius, $r > r_h$ are already trapped. The evolution therefore proceeds from a higher r to lower r and eventually zero. Once again the case where $D = 3$ is anomalous. One can see in the above plot that the MTS never reaches less than a particular value of comoving coordinate r. The reason is that for the case of $2 + 1$ dimensions not all shells can get trapped [24]. In the case of negative cosmological constant, there is a mass gap that needs to be filled before the shells can get trapped. So the shells closer to $r = 0$ do not get trapped. In the next plot, we see that all these shells that do not get trapped, do become singular due to their physical radius R becoming zero. The expression for R is

$$-\sqrt{\frac{n(n+1)}{2\Lambda}} \tan\left(\sqrt{\frac{\Lambda(n+1)}{2n}}t - \arcsin\sqrt{\frac{\Lambda}{g}}\right) \quad (62)$$

and the plot for R versus t is shown in Fig. 4.
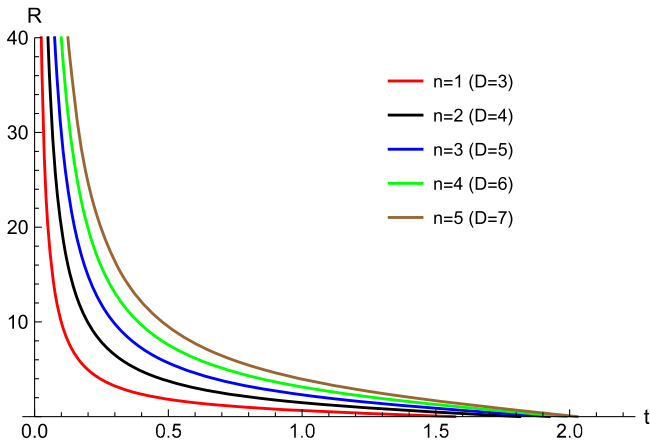
FIG. 4. R versus t for MTT with ($\Lambda = 1$, $g = 1$).

As can be seen from Eq. (47), the MTT is spacelike for $D \geq 5$. Timelike behavior is possible only in dimension less than 5. Any MTS that occurs at a areal radius less than $R < \sqrt{n(3-n)/|\Lambda|}$ is timelike and for $R > \sqrt{n(3-n)/|\Lambda|}$ it is spacelike. We can see that the above statement is covariant since the areal radius can be defined in a covariant manner based on the Killing vectors. We note that the area of the MTS in the negative cosmological constant case decreases monotonically with the coordinate time t for all the cases irrespective of the number of dimensions and whether the MTS is spacelike, timelike or mix of timelike and spacelike segments.

We now look at the classification of outer/ inner based on the expression $\pounds_l\Theta_k = n(3 - n + 2\Lambda R^2/n)/2R^2$. For $\Lambda < 0$, it is clear that for $D \geq 5$ the horizon is uniformly outer since the above expression is uniformly negative, it is therefore FOTH. For $D < 5$ it is an FOTH at large R and is FITH for small R. So there is a change from outer to inner as the horizon evolves. This counterintuitive behavior is addressed in the note at the end of the section.
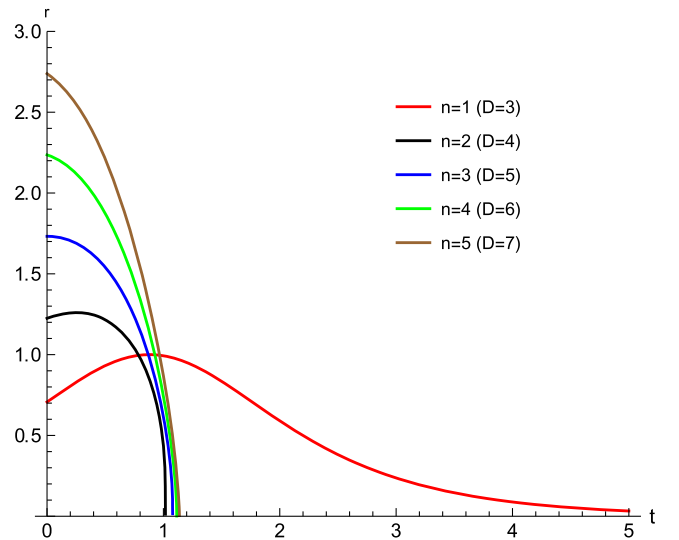
3. MTS for dS case

The solution for scaling $a(t)$ with positive cosmological constant for MTS is chosen to be (this is choice is made such that r, R are positive)

$$\left(-\sqrt{\frac{g}{\Lambda}}\sinh\left(\sqrt{\frac{\Lambda(n+1)}{2n}}t - arc\sin h\sqrt{\frac{\Lambda}{g}}\right)\right)^{\frac{2}{n+1}}. \quad (63)$$

The expression for the MTT curve in (r, t) is plane is give by comoving radius r which is

$$-\sqrt{\frac{n(n+1)}{2\Lambda}}\frac{1}{a(t)}\tanh\left(\sqrt{\frac{\Lambda(n+1)}{2n}}t - \text{arcsinh}\sqrt{\frac{\Lambda}{g}}\right). \quad (64)$$

The plot for r versus t is shown in Fig. 5.

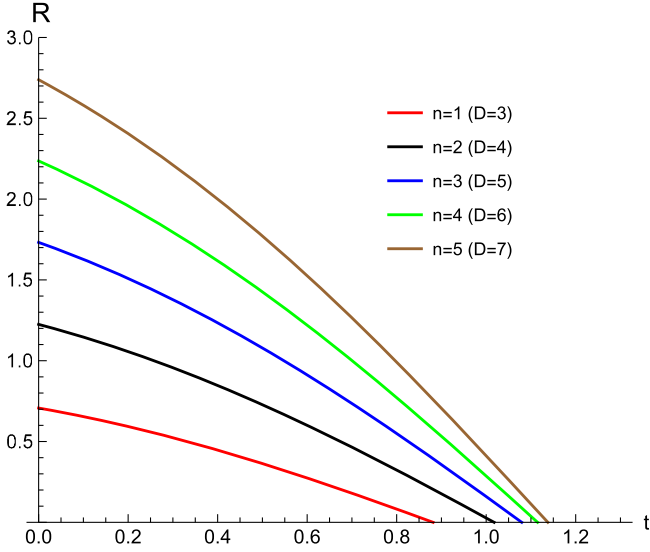FIG. 5. r versus t for MTT with ($\Lambda = 1$, $g = 1$).

FIG. 6. R versus t for MTT with ($\Lambda = 1, g = 1$).

Just like flat and AdS cases, the curve for the case when $D = 3$ is an anomaly. We look at the expression for the areal radius R of the MTT curve which is

$$-\sqrt{\frac{n(n+1)}{2\Lambda}} \tanh \left(\sqrt{\frac{\Lambda(n+1)}{2n}} t - \mathrm{arcsinh} \sqrt{\frac{\Lambda}{g}} \right) \quad (65)$$

The plot for R versus t is shown in Fig. 6.

We see from the above graphs that just like flat and negative cosmological constant cases, the evolution of MTS for positive cosmological constant case is also monotonic and the areal radius decreases monotonically with time t. Using the formula (47), we see that for dimensions $d \geq 5$, the MTS is timelike whenever $R > \sqrt{n(3-n)/(2\Lambda)}$ and is spacelike when $R < \sqrt{n(3-n)/(2\Lambda)}$. For dimension $D < 5$, the MTS hypersurface is timelike since the norm is always positive.

When we analyze the plot (r, t) and (R, t) together for the case of $D = 3$ dimensions, we see that the portion of the curve in (r, t) plot where the slope is positive is the relevant portion. The peak and the downward portion is a result of extending the curve beyond the singularity. This can be seen because when we observe the plot (R, t), we can see that the MTS has reached $R = 0$ while the curve in the (r, t) plot is still climbing. The anomalous behavior of the curve in the (r, t) plane is due to the fact that in $D = 3$ dimensions, particles do not attract each other while the positive cosmological constant has a repulsive effect on the evolving dust. So if a shell of comoving radius r is such that it's $\dot{R} = -1$ and therefore it is a point on the MTS curve. Due to the repulsive nature of positive cosmological constant, the shell of label r slows down so that it's $\dot{R} > -1$ and a shell with larger comoving radius will

have $\dot{R} = -1$. This explains the peculiar behavior of the $D = 3$ curve. This differs from other dimensions where the evolution of dust is not just dependent on the cosmological constant but also matter distribution that is attractive in nature.

To characterize the MTS in terms of outer and inner, we look at the sign of $\pounds_l \Theta_k = n(3 - n + 2\Lambda R^2/n)/2R^2$. We see that for dimension $D \leq 5$, the sign is uniformly positive implying that the horizon is an inner horizon (FITH). For $D > 5$, the horizon is inner horizon (FITH) for large R and is outer horizon (FOTH) for small R.

C. Marginally antitrapped surfaces (MATS)

The condition for marginally outer trapped surfaces is

$$\theta_+ > 0 \quad \text{and} \quad \theta_- = 0. \quad (66)$$

These conditions imply

$$\dot{R} = 1 \quad \text{and} \quad dotR > -1 \quad (67)$$

when $\dot{R} = 1$ we can write co.moving radius as function of time as

$$r = \frac{1}{\dot{a}(t)} \quad (68)$$

and the physical radius is expressed as

$$R(t, r) = \frac{a(t)}{\dot{a}(t)}. \quad (69)$$

We will look at the behavior of MATS for the cases where $\Lambda = 0, > 0$, and < 0.
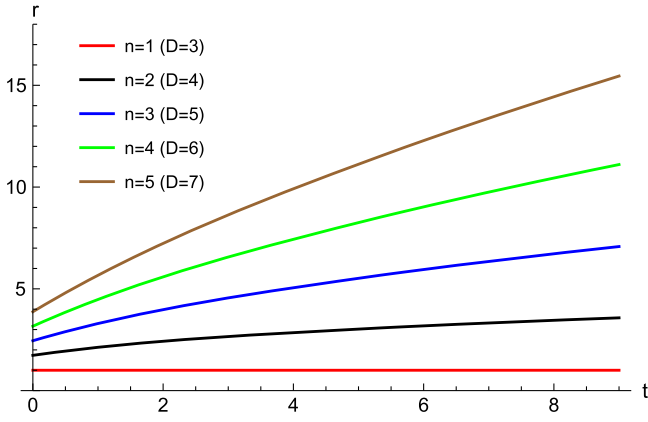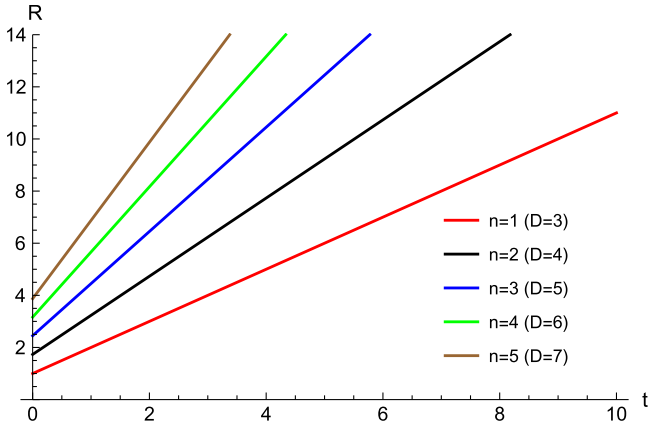
1. MATS for flat case

The solution for the case of expanding cloud of dust is given by,

$$a(t) = \left(1 + \sqrt{\frac{g(n+1)}{2n}} t \right)^{\frac{2}{1+n}} \quad (70)$$

we obtain r as a function of time given by

$$\sqrt{\frac{n(n+1)}{2g}} \left(1 + \sqrt{\frac{g(n+1)}{2n}} t \right)^{\frac{n-1}{1+n}}. \quad (71)$$

The plot for r versus time for the above relation is shown in Fig. 7.

FIG. 7. r versus t for MATT with ($\Lambda = 0$, $g = 1$).

FIG. 8. R versus t of MATT with ($\Lambda = 0$, $g = 1$).

Then the expression for the physical radius R for the MATS curve is

$$\sqrt{\frac{n(n+1)}{2g}} + \frac{(n+1)t}{2}. \quad (72)$$
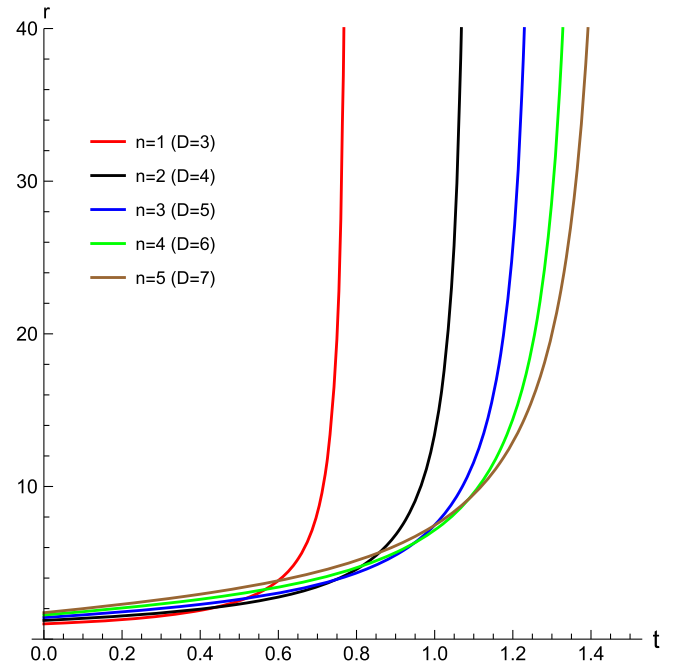
The plot for R versus t is shown in Fig. 8.

We see a monotonic evolution of R with time. Just as with MTT, the MATT curve is timelike for dimension $D < 5$, is null for $D = 5$ and is spacelike for $D > 5$.

The MATS could also be further characterized based on the sign of (51) from which we can see that for $D < 5$ the horizon is inner (PITH) and for $D > 5$ the horizon is outer (POTH).

2. MATS for AdS case

The solution for the scale factor $a(t)$ as a function of time for the case with a negative cosmological constant is obtained below (the choice is made such that r, R are positive)

FIG. 9. r versus t of MATT with ($\Lambda = 1$, $g = 1$).

$$\left(\sqrt{\frac{g}{\Lambda}} \sin \left(\sqrt{\frac{\Lambda(n+1)}{2n}} t + \arcsin \sqrt{\frac{\Lambda}{g}} \right) \right)^{\frac{2}{n+1}}. \quad (73)$$

The expression for comoving radius r is

$$\sqrt{\frac{n(n+1)}{2\Lambda}} \frac{1}{a(t)} \tan \left(\sqrt{\frac{\Lambda(n+1)}{2n}} t + \arcsin \sqrt{\frac{\Lambda}{g}} \right). \quad (74)$$

The plot for r versus t is shown in Fig. 9.
The expression for areal radius R is

$$\sqrt{\frac{n(n+1)}{2\Lambda}} \tan \left(\sqrt{\frac{\Lambda(n+1)}{2n}} t + \arcsin \sqrt{\frac{\Lambda}{g}} \right) \quad (75)$$

and the plot for R versus t is shown in Fig. 10.

One sees that the solutions $a(t)$ are oscillatory in nature. We consider the expanding part of the solution and track the evolution of MATS. The cloud expands to a maximum and starts contracting back in a finite comoving time t. The steep slope of the MATS curve owes its explanation to the previous sentence.

Just like MTS, for dimension $D < 5$, the MATS curve transitions from timelike for small R to spacelike for large R. For $D \geq 5$, the curve is uniformly spacelike. When we look at the sign of (51), we conclude that for $D < 5$ the
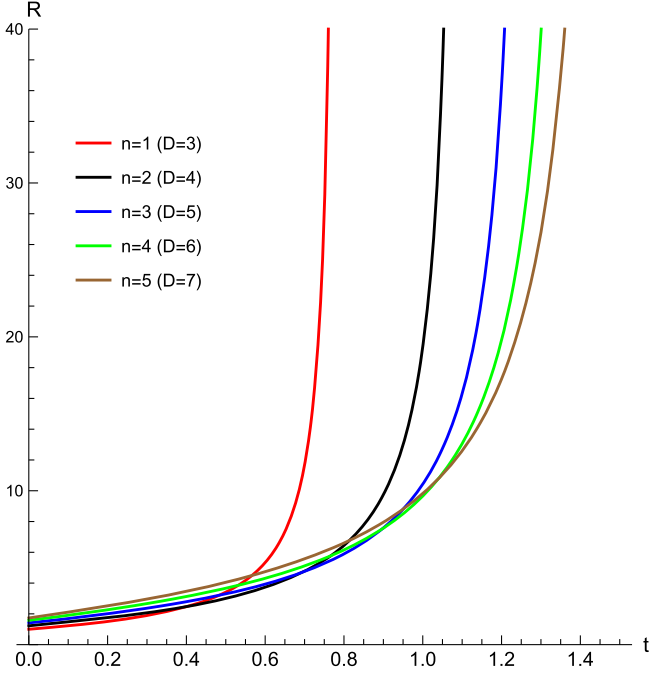
FIG. 10. R versus t of MATT with ($\Lambda = 1$, $g = 1$).

horizon is a PITH for small R and POTH for large R and for dimensions $D \geq 5$, the horizon is POTH.

3. MATS for dS case

The solution for the scaling factor $a(t)$ for MATS in positive cosmological constant is

$$\left(\sqrt{\frac{g}{\Lambda}} \sinh \left(\sqrt{\frac{\Lambda(n+1)}{2n}}t + \operatorname{arcsinh}\sqrt{\frac{\Lambda}{g}} \right) \right)^{\frac{2}{n+1}}. \quad (76)$$

The expression for r for MATS is

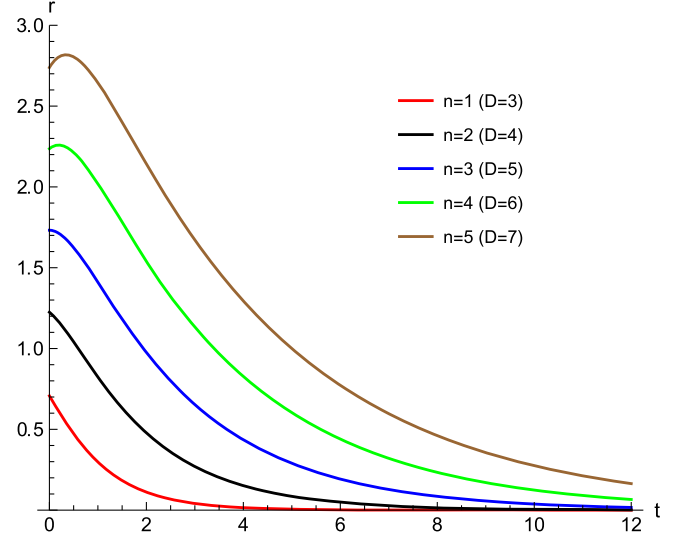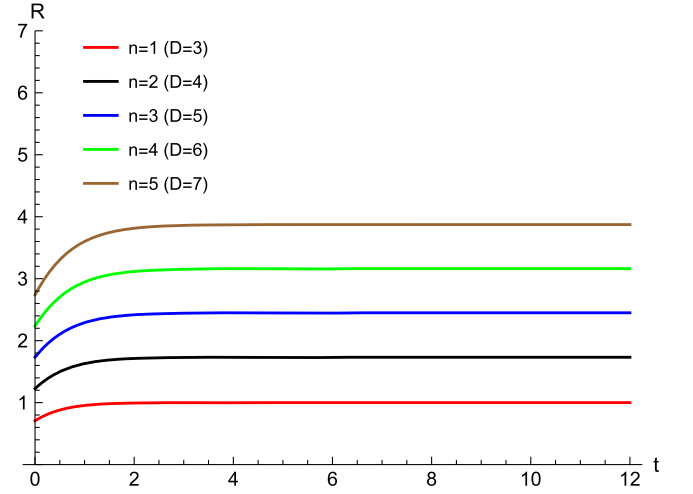$$\sqrt{\frac{n(n+1)}{2\Lambda}} \frac{1}{a(t)} \tanh \left(\sqrt{\frac{\Lambda(n+1)}{2n}}t + \operatorname{arcsinh}\sqrt{\frac{\Lambda}{g}} \right) \quad (77)$$

and the plot for r versus t is shown in Fig. 11.

and the expression for areal radius R as a function of time is

$$\sqrt{\frac{n(n+1)}{2\Lambda}} \tanh \left(\sqrt{\frac{\Lambda(n+1)}{2n}}t + \operatorname{arcsinh}\sqrt{\frac{\Lambda}{g}} \right) \quad (78)$$

the plot for R versus time for MATS evolution is shown in Fig. 12.

FIG. 11. r versus t for MATT with ($\Lambda = 1$, $g = 1$).

FIG. 12. R versus t for MATT with ($\Lambda = 1$, $g = 1$).

From the expression (47) it is clear that if $D \leq 5$ the curve is timelike and is a PITH. As is well known from various work on cosmological horizons in 4 dimensions regarding horizon evolution due to flux of matter [6]. For dimension $D > 5$ we have MITS curve is spacelike (also POTH) for small R (whenever $R < \sqrt{n(3-n)/(2\Lambda)}$) and is timelike (also PITH) for $R > \sqrt{n(3-n)/(2\Lambda)}$. Just like MTS, there is a transition from spacelike to timelike as the MATS evolves. As can be observed from the above plots, R evolves monotonically with time t. The plot R vs t is horizontal for large time t. This is because most of the matter interior to the MATS surface has crossed the "cosmological horizon" and therefore the flux of matter is negligible thereof.

D. Note: Outer and inner horizon classification criteria for $D = 5$ and monotonicity of horizon evolution

In this note, we elaborate on two separate points from the results on the section on MTS and MATS. The first point is the classification of inner and outer for the case of $D = 5$ with zero cosmological constant. We have seen that the horizon is uniformly null but not isolated. This is seen for both the MTS and MATS case. Now in order to classify the horizon in terms of being outer or inner, we can check with the Lie derivatives $\pounds_l \Theta_k$ and $\pounds_k \Theta_l$ (48), (49), (50), (51), both are indeed zero. In such situations, we propose another criteria to characterize the outer or inner nature of the horizon.

The classification is made possible by defining a space-like vector given by $\epsilon = \partial/\partial R$ in a coordinate chart (t, R, θ, ϕ) where t is the comoving time. The vector $\partial/\partial t$ is everywhere timelike a good time coordinate everywhere except at curvature singularity. Now ϵ points in the direction of increasing areal radius. We can now construct the quantities, $\pounds_\epsilon \Theta_k$ for MTS and $\pounds_\epsilon \Theta_l$ for MATS. The horizon is outer if $\pounds_\epsilon \Theta_k$ is positive and inner if $\pounds_\epsilon \Theta_k$ is negative for MATS. Similarly, the horizon is Outer if $\pounds_\epsilon \Theta_l < 0$ and Inner if $\pounds_\epsilon \Theta_l > 0$. The use of the vector ϵ is limited to the case when the MTT or MATT is null. The reason for this is that if the horizon is for space-like, then the expression of the type $\pounds_\epsilon \Theta_k$ can have variable sign (depending on the time coordinate being used) even though $\pounds_l \Theta_k$ has an invariant sign.

Evaluating the expression $\pounds_\epsilon \Theta_k$, we obtain the general expression for $D = 5$ with zero cosmological constant,

$$\pounds_\epsilon \theta_k = \frac{3}{R^2}\left[2 - \frac{F'}{R'R}\right] \tag{79}$$

Using the results (44), (46) for $D = 5$ we obtain, $\pounds_\epsilon \theta_k = -6/R^2$, which means we have an inner horizon. Similarly, we can classify MATS for the $D = 5$ as an inner horizon. We note that we can reach the same conclusion if we used the space-like vector field to be $\partial/\partial r$ in the comoving coordinate chart (t, r, θ, ϕ) coordinates system (with the additional assumption that $R' > 0$ and therefore r and R are monotonically increasing functions of each other).

The second point that is the observation that in the presence of a cosmological constant, the horizon evolution makes a transition from timelike to spacelike as is observed in deSitter case for dimension $D > 5$. We note that for larger R, the horizon is timelike and small R it is spacelike. What seems nontrivial in these cases is that when one classifies the horizon as an inner or outer horizon, one encounters the following situation that as long as the curve is timelike the horizon is an inner surface whereas in the spacelike segment it is an outer surface. When we see the plots for the horizon evolution, we see a monotonic decrease in the areal radius R for both the timelike and spacelike segments of the curve. The transition from inner surface to outer surface is counterintuitive. The analysis of such curves has been done rigorously in [11,12]. The understanding is that for the spacelike segment of the curve that decreases monotonically with the coordinate t, one can show that for a different choice of coordinates, the time ordering of the events of the spacelike segment can be reversed. So in this coordinate system, the spacelike part of the horizon evolves from $R = 0$ with an increasing area (since it is outer and therefore FOTH) and meets the timelike segment of the curve at the radius R (where the curves in the plots transition from timelike to spacelike).

IV. AREA LAWS IN MARGINALLY TRAPPED SURFACES

The area law for a dynamical horizon (codimension 1 spacelike surface) and a timelike membrane (codimesion 1 timelike surface) in $3 + 1$ dimensions is given by Abhay Ashtekar and Badri Krishnan [5,6]. They obtained an area balance law for the dynamical horizon which is

$$\left(\frac{R_2}{2G} - \frac{R_1}{2G}\right) = \int_{\Delta H} \overline{T}_{ab} \hat{\tau}^a \xi^b_{(r)} d^3 v$$
$$+ \frac{1}{16\pi G}\int_{\Delta H} N_r(|\sigma^2| + 2|\zeta|^2) d^3 v. \tag{80}$$

The two terms on the right-hand side are the matter energy flux and the gravitational energy flux along the evolution vector $\xi^b_{(r)}$ and similarly the area balance law for the timelike membrane is

$$\left(\frac{R_2}{2G} - \frac{R_1}{2G}\right) = -\int_{\Delta H} \overline{T}_{ab} \hat{r}^a \xi^b_{(t)} d^3 v$$
$$- \frac{1}{16\pi G}\int_{\Delta H} N_t(|\sigma^2| - 2|\zeta'|^2) d^3 v. \tag{81}$$

Using these area laws they have also argued that the area increases for dynamical horizons and decreases for timelike membrane monotonically.

Following there derivation of area laws closely we look to extend these laws for marginally (anti) trapped yubes which are spacelike codimension 1 hyper-surfaces to a higher dimensional spacetime $(D = n + 2)$ with a topology of $\mathbb{R}^2 \times \mathbb{S}^d$. For a codimension-1 foliation of the spacetime, specifying the evolution vector field ξ^a will also specify the lapse function and shift vectors in the $1 + (n + 1)$ decomposition.

$$N\tau^a + N^a = \xi^a \tag{82}$$

H is a MTT and is a codimension-1 hypersurface with the Cauchy data and there constraint equations are

$$C(q, k) := R + k^2 - K^{ab}K_{ab} = 2\kappa \overline{T}_{ab}\tau^a \tau^b \tag{83}$$

$$C^a(q,k) := D_b(K^{ab} - Kq^{ab}) = \kappa \overline{T}^{bc}\tau_c q_b^a \quad (84)$$

where $\overline{T}_{ab} = T_{ab} - (\Lambda g_{ab}/\kappa)$ and τ^a is the unit normal to H. To get the flux through the a region of MTT (ΔH) bounded by two marginally trapped surfaces at different times we need to evaluate

$$\int_{\Delta H}(NC + N_a C^a)d^{n+1}v \quad (85)$$

using the Eqs. (83) and (84) we have

$$\int_{\Delta H}(NC + N_a C^a)d^{n+1}v$$
$$= 2\kappa \int_{\Delta H}(N\overline{T}_{ab}\tau^a\tau^b + 2N_a\overline{T}^{bc}\tau_c q_b^a)d^{n+1}v. \quad (86)$$

For a MTT the choice of the evolution vector field is $\xi^a = Nk^a$ and a further $1 + n$ decomposition of H with Σ as a MTS which is a codimension-2 hypersurface with a topology of $\mathbb{S}^n$. With this setup and following the steps as in [5] we end up with a similar equation as (3.21) in [5]

$$\int_{\Delta H}N\tilde{R}d^{n+1}v = 2\kappa\int_{\Delta H}\overline{T}_{ab}\xi^a\tau^b d^{n+1}v$$
$$+ \int_{\Delta H}N(|\sigma|^2 + |\zeta|^2)d^{n+1}v. \quad (87)$$

The quantities in the gravitational flux energy term are defined below. The shear for the outgoing bundle of light rays is

$$\sigma_{ab}^k = \left(h_a^c h_b^d - \frac{1}{2}h_{ab}h^{cd}\right)\nabla_c k_d \quad (88)$$

where h_b^a is the projection operator onto the n-sphere and is given by

$$h_b^a = \delta_b^a - l_b l^a - k^a k_b \quad (89)$$

computing the norm of the shear for outgoing null rays we get

$$|\sigma^k|^2 = \sigma_{ab}^k \sigma^{kab} = \frac{n(n-2)^2}{4}\frac{e^{-\lambda}(R' + e^{(\frac{\lambda}{2})}\dot{R})^2}{R^2} \quad (90)$$

and using the condition 28 for MTS we can see that the norm of the shear for outgoing null rays is zero. Similarly the shear for the ingoing bundle of null rays is

$$\sigma_{ab}^l = \left(h_a^c h_b^d - \frac{1}{2}h_{ab}h^{cd}\right)\nabla_c l_d \quad (91)$$

and computing the norm of the shear for ingoing null rays we get

$$|\sigma^l|^2 = \sigma_{ab}^l \sigma^{lab} = \frac{n(n-2)^2}{4}\frac{e^{-\lambda}(R' - e^{(\frac{\lambda}{2})}\dot{R})^2}{R^2} \quad (92)$$

and using the condition (29) for MATS we see that the shear norm go to zero. The quantity ζ for MTT is given by the expression

$$\zeta^a = s^{ab}r^a\nabla_c k_b \quad (93)$$

where s^{ab} is the intrinsic metric on MTS. One can easily check that for a spherical symmetry the norm $|\zeta|^2$ is always zero for both the MTS and the MATS. We can see that for spherical dust evolution the gravitational wave energy term always vanishes. Hence the only contribution for the change in marginally trapped surfaces comes from the matter energy flux.

The volume element on the MTT (H) can be written as $d^{n+1}v = N^{-1}dRd^n v$ so the expression (87) reduces to

$$\int_{R_1}^{R_2}dR\oint_{S^n}\tilde{R}d^n v = 2\kappa\int_{\Delta H}(N\overline{T}_{ab}l^a\tau^b)d^{n+1}v. \quad (94)$$

The n-dimensional volume element on $\mathbb{S}^n$ is $d^n v = R^n \sin\theta_1 \sin^2\theta_2 ....\sin^{n-1}\theta_{n-1}d\theta d\theta_1 d\theta_2 ....d\theta_{n-1}$ and Ricci scalar $\tilde{R}$ for the n-sphere is $\tilde{R} = n(n-1)/R^2$, where R is the areal radius. So volume integral of Ricci scalar for the n-sphere is

$$\oint_{S^n}\tilde{R}d^n v = \frac{2\pi^{(\frac{n+1}{2})}n(n-1)R^{n-2}}{\Gamma(\frac{n+1}{2})} \quad (95)$$

and the area of the n-sphere with radius R is given by

$$A(R) = \frac{2\pi^{(\frac{n+1}{2})}R^n}{\Gamma(\frac{n+1}{2})}. \quad (96)$$

The left-hand side of the integral (94) becomes

$$\int_{R_1}^{R_2}dR\oint_{S^n}\tilde{R}d^n v = \frac{2\pi^{(\frac{n+1}{2})}n}{\Gamma(\frac{n+1}{2})}(R_2^{n-1} - R_1^{n-1}). \quad (97)$$

For evaluating the matter flux term of the equation (94) we use the relation $d^{n+1}v = N^{-1}dRd^n v$ again and also (11) which simplify the expression as

$$2\kappa\int_{\Delta H}\left(N\left(T_{ab} - \frac{\Lambda g_{ab}}{k}\right)l^a\tau^b\right)d^{n+1}v$$
$$= 2\frac{2\pi^{(\frac{n+1}{2})}}{\Gamma(\frac{n+1}{2})}\int_{\Delta R}\left(\frac{nF'}{2R^n R'} + \Lambda\right)R^n dR. \quad (98)$$

Now the expression (94) reduces to the form

$$\int_{\Delta R} n(n-1)R^{n-2}dR - 2\Lambda \int_{\Delta R} R^n dR = n \int_{\Delta r} F'dr.$$

Upon integration we have the relation

$$(R_2^{n-1} - R_1^{n-1}) - \frac{2\Lambda}{n(n+1)}(R_2^{n+1} - R_1^{n+1})$$
$$= F(r_2)_{R_2} - F(r_1)_{R_1} \qquad (99)$$

where the subscript R_2 or R_1 indicates the value of R where $F(r)$ needs to be evaluated at. The above expression therefore is,

$$\Delta R^{n-1} - \frac{2\Lambda}{n(n+1)}\Delta R^{n+1} = \Delta F(r). \qquad (100)$$

This is same as the relation (10) under the marginally (anti) trapped condition $\dot{R}^2 = 1$ which is either $\dot{R} = -1$ ($\Theta_k = 0$) and $\dot{R} = 1$ ($\Theta_l = 0$). Note that the area balance law has been reduced to an algebraic relation between the misner-sharp mass $F(r)$ and the area radius R. Also this extension to D-dimensional area balance law is done for only spacelike MTS or MATS.

V. CONCLUSIONS

We have generalized the evolution of MTS and MATS in D-dimensions with and without the cosmological constant due to the evolution of pressure-less matter. The model under consideration is simple enough to yield closed form expressions for various aspects of the horizon evolution in these space-times and general enough to capture the various scenarios possible. This advantage makes this model particularly useful in the study of entropy evolution and quantum gravity scenarios. Particularly interesting result among them is the formula for the causal nature of the horizon. The formula highlights the dependence on dimension, local energy density, cosmological constant and the area radius (D-dimensional generalization of area).

The analysis of MTS and MATS in D-dimensions yields many results that are not a straightforward extension of the results of $3 + 1$ dimensions. We observe that the qualitative features of the dynamics of the horizons depends crucially on the number of dimensions D. In the examples that were shown, there were cases where MTS and MATS were uniformly null but not isolated and moreover the area evolves monotonically with the comoving time. We have also shown that the generalization of Oppenheimer-Snyder model in D-dimensions yields the horizon to be timelike for dimension $D < 5$ and is spacelike for $D > 5$. This is interesting since the area monotonically decreases with co-moving time in-spite of the horizon being spacelike, timelike in different segments of the same curve. These results make the analysis in d-dimensions counter-intuitive. When we consider the case of Homogeneous distribution of dust, we obtain the result that whenever the segment of the MTS or MATS curve that is at an area radius $R < R_{\text{critical}}$, ($R_{\text{critical}} = \sqrt{n(3-n)/(2\Lambda)}$), the curve is timelike and for $R > R_{\text{critical}}$ it is spacelike. When one explores the expression for R_{critical}, we see that it depends only on dimension and cosmological constant Λ. The length scale of this partitioning of Area radius is decided solely by the cosmological constant. The details of the transitions across R_{critical} can yield very interesting result and are left for future considerations.

We have found expressions for the Ashtekar, Badrikrishnan's area balance law in D-dimensions for a restricted class of $\mathbb{S}^n$ topologies that are relevant for the model under consideration. The expressions obtained in the article are valid for the Dynamical Horizons. One can extend the expressions for the case of timelike membranes too (as is shown in the paper Ashtekar et al. [6]). In the cases considered we show that the horizon transitions from timelike to spacelike during the course of evolution. The generalization of the $3 + 1$ of [6] where such transitions are allowed will be attempted in a later work.

[1] R. Penrose, Gravitational Collapse and Space-Time Singularities, Phys. Rev. Lett. **14**, 57 (1965).

[2] S. A. Hayward, General laws of black-hole dynamics, Phys. Rev. D **49**, 6467 (1994).

[3] A. Ashtekar, C. Beetle, O. Dreyer, S. Fairhurst, B. Krishnan, J. Lewandowski, and J. Wiśniewski, Generic Isolated Horizons and their Applications, Phys. Rev. Lett. **85**, 3564 (2000).

[4] A. Ashtekar, S. Fairhurst, and B. Krishnan, Isolated horizons: Hamiltonian evolution and the first law, Phys. Rev. D **62**, 104025 (2000).

[5] A. Ashtekar and B. Krishnan, Dynamical Horizons: Energy, Angular Momentum, Fluxes, and Balance Laws, Phys. Rev. Lett. **89**, 261101 (2002).

[6] A. Ashtekar and B. Krishnan, Dynamical horizons and their properties, Phys. Rev. D **68**, 104030 (2003).

[7] A. Ashtekar and B. Krishnan, Isolated and dynamical horizons and their applications, Living Rev. Relativity **7**, 10 (2004).

[8] I. Booth, L. Brits, J. A. Gonzalez, and C. Van Den Broeck, Marginally trapped tubes and dynamical horizons, Classical Quantum Gravity **23**, 413 (2005).

[9] O. Dreyer, B. Krishnan, D. Shoemaker, and E. Schnetter, Introduction to isolated horizons in numerical relativity, Phys. Rev. D **67**, 024018 (2003).

[10] R. Bousso, Holography in general space-times, J. High Energy Phys. 99 (1999) 028.

[11] R. Bousso and N. Engelhardt, New Area Law in General Relativity, Phys. Rev. Lett. **115**, 081301 (2015).

[12] R. Bousso and N. Engelhardt, Proof of a new area law in general relativity, Phys. Rev. D **92**, 044031 (2015).

[13] R. Tibrewala, S. Gutti, T. P. Singh, and C. Vaz, Classical and quantum gravitational collapse in d-dimensional ads spacetime: Classical solutions, Phys. Rev. D **77**, 064012 (2008).

[14] A. M. Sherif, R. Goswami, and S. D. Maharaj, Some results on cosmological and astrophysical horizons and trapped surfaces, Classical Quantum Gravity **36**, 215001 (2019).

[15] A. Helou, I. Musco, and J. C. Miller, Causal nature and dynamics of trapping horizons in black hole collapse, Classical Quantum Gravity **34**, 135012 (2017).

[16] A. Helou, Dynamics of the four kinds of trapping horizons and existence of hawking radiation, arXiv:1505.07371.

[17] S. A. Hayward, Energy and entropy conservation for dynamical black holes, Phys. Rev. D **70**, 104027 (2004).

[18] I. Booth, Black-hole boundaries, Can. J. Phys. **83**, 1073 (2005).

[19] I. Bengtsson and J. M. M. Senovilla, Region with trapped surfaces in spherical symmetry, its core, and their boundaries, Phys. Rev. D **83**, 044012 (2011).

[20] J. M. M. Senovilla, Singularity theorems and their consequences, Gen. Relativ. Gravit. **30**, 701 (1998).

[21] J. M. M. Senovilla, On the existence of horizons in spacetimes with vanishing curvature invariants, J. High Energy Phys. 03 (2003) 046.

[22] J. M. M. Senovilla, Novel results on trapped surfaces, arXiv:gr-qc/0311005.

[23] B. Grado-White and D. Marolf, Marginally trapped surfaces and ads/cft, J. High Energy Phys. 18 (2018) 49.

[24] S. Gutti, Gravitational collapse of inhomogeneous dust in $(2 + 1)$ dimensions, Classical Quantum Gravity **22**, 3223 (2005).

[25] R. B. Mann and S. F. Ross, Gravitationally collapsing dust in $2 + 1$ dimensions, Phys. Rev. D **47**, 3319 (1993).